Peierls Stress for an Idealized Crystal Model*

W. T. SANDERS
Department of Mechanical Engineering, Columbia University, New York, New York
(Received April 27, 1962; revised manuscript received July 18, 1962)

An analytical investigation is made of the geometry of an edge dislocation in a simple atomic model of an infinite crystal, and the effect on the dislocation of externally applied shear stress. This study indicates that in dislocation theory significant results may be obtained from the discrete model, on which accurate analysis is possible. Even the simple model used here seems to be sufficiently realistic to yield meaningful results.

The width, w, of the dislocation, in this model, is proportional to γ^{-1}, where γ is the shear strength of a perfect crystal. The Peierls-Nabarro (P-N) stress has a large cyclic variation as γ is changed, but is proportional, in the average, to e^{-w}. This differs markedly from the result, $\sigma_{PN} \propto e^{-4\pi w}$, found from the continuum analysis. The values of the P-N stress ranged from 10^{-3} to 10^{-5}, in units of the shear modulus.

In the analysis, the doubly infinite set of difference equations, derived from force balances on the atoms, is first reduced, by a type of Fourier series transform, to an infinite system of equations, which is then solved by the method of reduction. Numerical results were obtained from the IBM 1620 digital computer. The over-all error in the P-N stress for this model is believed to be less than 10^{-6}.

1. INTRODUCTION

DISLOCATION theory is generally based on the analysis of continuum, or pseudocontinuum, models.[1] Even the calculation of an effect, such as the Peierls-Nabarro stress, that depends for its existence on the atomic nature of the crystal, has been made with only a slight modification to the continuum technique.

The Peierls-Nabarro (P-N) stress is generally defined as the minimum shear stress required to move a straight line dislocation through an otherwise perfect crystal, in the absence of thermal motion and with the dislocation line constrained to remain straight. The P-N stress is basic to the theory and would, if it were large enough compared with other forces, affect all other characteristics of the dislocation. The width of the dislocation is similarly basic, and yet neither of these properties has been successfully measured by direct experiment. Indirect experimental determination of the P-N stress, for which the nature of the assumed model is crucial, have indicated values ranging from 10^{-3} (in multiples of the shear modulus),[2-4] which, if correct, would mean this stress is certainly significant, down to 10^{-5} or less.[5]

This uncertainty, and possible importance, requires that theoretical analysis be attempted, at least to estimate order of magnitude. Peierls, in 1940, made the original calculation[6]; Nabarro, in 1947, corrected this,[7] and other workers[8-11] have tried, by making certain modifications, to refine the analysis.[12] In all this work, however, certain assumptions were made concerning the behavior of the models (apart from the assumptions implicit in the use of a model to represent reality) that could affect the result drastically, and that could not be verified on the basis of the models.[13]

The purpose of the present work has been to determine whether this calculation can be made using a completely atomistic model. The simplest reasonable model that would demonstrate the desired characteristics was chosen, and it was found that the dislocation geometry, the kinematics of its motion, and the P-N stress, for this particular model, could be determined accurately. Moreover the techniques found useful in the analysis are not limited to this model, but can be extended to cover more realistic features.

The widths of the dislocations, in this model, were found to be approximately the same as those calculated by Foreman, Jaswon, and Wood.[9] The P-N stress, for the same width, is roughly the same as that determined by Peierls[6] and Nabarro,[7] but the dependence on width, given approximately by $\sigma_{PN} \propto e^{-w}$, causes this stress to be several orders of magnitude greater, for wider dislocations, than that found by Foreman *et al.*[9]

In Sec. 2 of this paper the physical model, the method of introduction of the dislocation, and the mathematical problem to be solved are presented. The method of calculation of certain constants, and an outline of the procedure of solution is given in Sec. 3;

* This research was supported by the Air Force, through the Air Force Office of Scientific Research under Contract No. AF49(638)-909, and is based on a dissertation submitted in partial fulfillment of the requirements for the degree of Doctor of Engineering Science in Mechanical Engineering at Columbia University.

[1] Two exceptions are the work of H. B. Huntington, J. E. Dickey, and R. Thomson [Phys. Rev. **100**, 1117 (1955)], in which the atomic distribution around a dislocation in an alkali-halide was calculated numerically, and the work of I. Babuška, E. Vitásek, and F. Kroupa [Czech. J. Phys. **10**, 488 (1960)], in which the displacements around a very rough dislocation model were calculated to illustrate a mathematical technique.

[2] J. Heslop and N. J. Petch, Phil. Mag. **1**, 866 (1956).

[3] H. Donth, Z. Physik **149**, 111 (1957).

[4] J. Lothe, Phys. Rev. **115**, 543 (1959).

[5] A. H. Cottrell, *Dislocations and Plastic Flow in Crystals* (Oxford University Press, New York, 1953), Article 6.

[6] R. Peierls, Proc. Phys. Soc. (London) **A52**, 34 (1940).

[7] F. R. N. Nabarro, Proc. Phys. Soc. (London) **A59**, 256 (1947).

[8] J. D. Eshelby, Phil. Mag. **40**, 903 (1949).

[9] A. J. Foreman, M. A. Jaswon, and J. K. Wood, Proc. Phys. Soc. (London) **A64**, 156 (1951).

[10] H. D. Dietze, Z. Physik **131**, 156 (1952).

[11] H. B. Huntington, Proc. Phys. Soc. (London) **B68**, 1043 (1955).

[12] The P-N stress determined in the first calculation was about 10^{-4}; most of the subsequent work has produced much lower figures. Kuhlmann-Wilsdorf, using a different approach, has suggested that the Peierls stress should be in the range 10^{-3} to 10^{-2}. See D. Kuhlmann-Wilsdorf, Phys. Rev. **120**, 773 (1960).

[13] For a critical summary of these assumptions, see the paper by Huntington (reference 11).

Sec. 4 contains a detailed presentation of the results and conclusions.

2. PHYSICAL MODEL AND MATHEMATICAL DESCRIPTION

The physical model chosen for this first calculation is based on a simple cubic lattice with nearest neighbor, linear, interaction, including central and noncentral forces. When used for a nearly perfect crystal (wave propagation, point imperfections), this has been called the Rosenstock-Newell model.[14–16] The basic model is modified in the neighborhood of the slip plane, to attempt to account for the large relative displacements in that region.

Figure 1 illustrates the way in which an edge dislocation could be introduced into the perfect crystal. In this figure the atoms are imagined to lie at the intersections of the lines, while the lines themselves represent the force connections between the atoms.

In Fig. 1(a), an infinite crystal has been separated along the slip plane, and each half has been subjected to a uniform shear. This figure also shows the way in which the rows and columns of atoms are numbered. If u_{ij} is the horizontal displacement of the atom in the i row and j column, measured from the strain-free state, then, in the configuration of Fig. 1(a),

$$\begin{aligned} &i>0: \quad u_{ij}{}^{\mathrm{I}}=(\tau b^2/k_2)(i-1); \\ &i<0: \quad u_{ij}{}^{\mathrm{I}}=(\tau b^2/k_2)(i+1), \end{aligned} \tag{2.1}$$

τ is the (externally applied) shear stress, so that τb^2, where b is the lattice constant, is the force applied to each boundary atom, and k_2 is a measure of the strength of the noncentral force. By comparison with the continuum,

$$k_2=c_{44}b=\mu b, \tag{2.2}$$

where $c_{44}=\mu$ is the shear modulus.

In Fig. 1(b) the extra half-plane of atoms, characteristic to the edge dislocation, has been introduced by imposing displacements on the atom rows adjacent to the slip plane, compressing that of the upper half-crystal and extending that of the lower. The displacements u_{ij} from the strain-free state are now

$$u_{ij}=u_{ij}{}^{\mathrm{I}}+u_{ij}{}^{\mathrm{II}}, \tag{2.3}$$

and, for the rows adjacent to the slip plane,

$$\begin{aligned} u_{1j}{}^{\mathrm{II}}&=-b/4, \quad j>0; \qquad u_{-1,j}{}^{\mathrm{II}}=b/4, \quad j\geqslant 0; \\ &=0, \quad j=0; \qquad\qquad =-b/4, \quad j<0. \\ &=b/4, \quad j<0; \end{aligned} \tag{2.4}$$

In Fig. 1(c) the strained half-crystals have been brought together, so that the vertical separation is again b, and so that the horizontal separation of opposing atoms is $\tau b^2/k_2$. This horizontal offset equals, according to Eq. (2.1), the shear strain in the dislocation-free crystal, and therefore equals the asymptotic strain at large distances from the center of the dislocation.

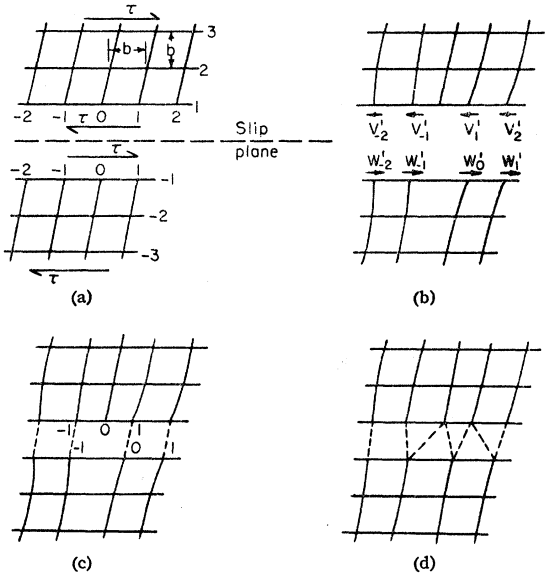

FIG. 1. Stages in dislocation formation. (a) Uniform shear stress τ is imposed on the separated half-crystals. (b) The boundary above the slip plane is compressed, that below extended by the forces V_j', W_j' (direction of arrows shows sign convention for positive forces). (c) The half-crystals are brought together, still constrained by externally applied forces. (d) Equilibrium position: Externally applied forces, except shear stress τ, are removed.

In Fig. 1(d) the constraints have been withdrawn and the atoms have been allowed to assume their equilibrium position. The final displacements, for the four rows nearest the slip plane, are now

$$\begin{aligned} u_{1j}&=u_{1j}{}^{\mathrm{I}}+u_{1j}{}^{\mathrm{II}}+\varphi_j', \quad u_{-1,j}=u_{-1,j}{}^{\mathrm{I}}+u_{-1,j}{}^{\mathrm{II}}+\psi_j', \\ u_{2j}&=u_{2j}{}^{\mathrm{I}}+u_{2j}{}^{\mathrm{II}}+\bar{\varphi}_j', \quad u_{-2,j}=u_{-2,j}{}^{\mathrm{I}}+u_{-2,j}{}^{\mathrm{II}}+\bar{\psi}_j', \end{aligned} \tag{2.5}$$

with $\varphi_j', \psi_j' \to 0$ as $|j|\to\infty$. The last statement follows from the fact that the configuration from which φ_j' and ψ_j' are measured [Fig. 1(c)] has the correct strain at infinity.

Near the center of the dislocation, the spacing between atoms on opposite sides of the slip plane departs radically from that in the perfect crystal. Consequently, in this region, the nearest-neighbor assumption is no longer justified, and each atom on the slip plane is considered to be connected, by lines of force, to two atoms on the opposite side [see Fig. 1(d)]. Each of these forces is taken to be a function of the horizontal distance between the two atoms so connected; from the definitions Eq. (2.5) [see also Fig. 1(c)] the required values of ϕ_{ij}, the distance between the i atom of the 1

[14] H. B. Rosenstock and G. F. Newell, J. Chem. Phys. **21**, 1607 (1953).
[15] E. W. Montroll and R. B. Potts, Phys. Rev. **100**, 525 (1955).
[16] R. F. Wallis, Phys. Rev. **116**, 302 (1959).

row and the j atom of the -1 row, are

$$\begin{aligned} i>0: &\quad \phi_{ii}=b-(\tau b^2/k_2)-\varphi_i'+\psi_i', \\ &\quad \phi_{i,i-1}=(\tau b^2/k_2)+\varphi_i'-\psi_{i-1}'; \\ i=0: &\quad \phi_{ii}=(3b/4)-(\tau b^2/k_2)-\varphi_0'+\psi_0', \\ &\quad \phi_{i,i-1}=(3b/4)+(\tau b^2/k_2)+\varphi_0'-\psi_{-1}'; \\ i<0: &\quad \phi_{ii}=-(\tau b^2/k_2)-\varphi_i'+\psi_i', \\ &\quad \phi_{i,i-1}=b+(\tau b^2/k_2)+\varphi_i'-\psi_{i-1}'. \end{aligned} \tag{2.6}$$

The equations governing the displacement distribution, in the region where the Rosenstock-Newell model is applicable, are derived from a force balance on a typical atom and are

$$k_1(u_{i,j+1}+u_{i,j-1}-2u_{ij}) +k_2(u_{i+1,j}+u_{i-1,j}-2u_{ij})=0, \tag{2.7}$$

where k_1 measures the strength of the central forces. Since inertial and other body forces are not considered, the left-hand side of the equation, which represents the net force on the atom due to surrounding atoms, is set equal to zero.

Equation (2.7) will be taken as valid for every atom except those in the 1 and -1 rows. Except for these rows on the slip plane, the nearest-neighbor model is consistent; the original spacing of nearest neighbors is b, and of next-nearest neighbors $b\sqrt{2}$, and since, as found *a posteriori*, the strain is everywhere less than 10%, the final spacing of nearest and next-nearest neighbors lies in the ranges $0.9b$ to $1.1b$ and $1.3b$ to $1.5b$, respectively, and clearly these ranges do not overlap.

Except for forces across the slip plane, the model is taken as linear, so that forces due to successive displacements may be added.

A convenient feature of the Rosenstock-Newell model is that the vertical and horizontal displacements are not coupled; Eq. (2.7) has no vertical displacement terms. Because of this, and the linearity, the horizontal displacements may be calculated independently of the vertical ones, provided the horizontal boundary forces or displacements are known. Finally, since the continuum calculations predict that the normal stress on the slip plane is zero, in the present calculations the forces acting across the slip plane are taken to be purely horizontal, and then the vertical displacements are everywhere zero.[17]

In the next section, influence coefficients k_j will be determined such that

$$u_{2j}=\sum_{-\infty}^{\infty} k_{j-k}u_{1k}, \quad u_{-2,j}=\sum_{-\infty}^{\infty} k_{j-k}u_{-1,k}.$$

That is, the displacements in the second rows may be related to those of the first. It follows from the linearity of the model that

$$u_{2j}^{\mathrm{II}}=\sum_{-\infty}^{\infty} k_{j-k}u_{1k}^{\mathrm{II}}, \quad \bar{\varphi}_j'=\sum_{-\infty}^{\infty} k_{j-k}\varphi_k', \text{ etc.} \tag{2.8}$$

In order to write force balances, analogous to Eq. (2.7), for the slip plane atoms, let F_{ij} be the force of attraction between the i atom in row 1 and the j atom in row -1; then

$$k_2(u_{2j}-u_{1j})+k_1(u_{1,j+1}+u_{1,j-1}-2u_{1j}) =F_{j,j-1}-F_{jj}, \tag{2.9a}$$

$$k_2(u_{-2,j}-u_{-1,j})+k_1(u_{-1,j+1}+u_{-1,j-1}-2u_{-1,j}) =F_{jj}-F_{j+1,j}. \tag{2.9b}$$

If the relations (2.5) are used in Eqs. (2.9), together with Eqs. (2.1), the following equations are derived:

$$k_2(\bar{\varphi}_j'-\varphi_j')+k_1(\varphi_{j+1}'+\varphi_{j-1}'-2\varphi_j') =-\tau b^2-V_j'+F_{j,j-1}-F_{jj}, \tag{2.10a}$$

$$k_2(\bar{\psi}_j'-\psi_j')+k_1(\psi_{j+1}'+\psi_{j-1}'-2\psi_j') =\tau b^2+W_j'+F_{jj}-F_{j+1,j}, \tag{2.10b}$$

where

$$V_j'=k_2(u_{2j}^{\mathrm{II}}-u_{1j}^{\mathrm{II}}) +k_1(u_{1,j+1}^{\mathrm{II}}+u_{1,j-1}^{\mathrm{II}}-2u_{1j}^{\mathrm{II}}), \tag{2.11a}$$

$$W_j'=-k_2(u_{-2,j}^{\mathrm{II}}-u_{-1,j}^{\mathrm{II}}) -k_1(u_{-1,j+1}^{\mathrm{II}}+u_{-1,j-1}^{\mathrm{II}}-2u_{-1,j}^{\mathrm{II}}). \tag{2.11b}$$

The quantities V_j' and W_j' can be seen to be the boundary forces necessary to produce the configuration of Fig. 1(b) from that of Fig. 1(a). Because of the linearity of the model they can be computed separately.

It remains to devise a relation connecting the force F_{ij}, acting across the slip plane, and the separation, ϕ_{ij}, of the two atoms involved. This relation must have at least the following three properties:

(1) The initial slope, $(\partial F_{ij}/\partial\phi_{ij})$ at $\phi_{ij}=0$, should equal k_2 in order to be consistent with the rest of the model for small strain.

(2) $F_{ij}(\phi_{ij})$ must have a maximum F_c for some $\phi_{ij}=\phi_c$ between 0 and b. This is both physically reasonable and necessary to allow the dislocation to move.

(3) The force should go to zero for some value of $\phi_{ij}<$b, to conform to the nearest neighbor property of the model.

The simplest relation with these properties, and the one chosen for this calculation, is made up of two linear segments, as shown in Fig. 2. For $\phi(=\phi_{ij})$ less than ϕ_c, the force $F(=F_{ij})$ is given by $F=k_2\phi$, in accordance with requirement (1) above. When the separation of two atoms is within this range, a "strong bond" will be said to exist between them. The maximum force F_c corresponds to the shear strength of the perfect crystal. The cutoff point is set at $\phi=b-\phi_c$, so that the

[17] The methods to be used do not depend on this property of the model, and a logical first improvement to the present calculation would be to include vertical and horizontal coupling both on the slip plane and in the interior.

second linear segment is necessarily $F=F_c[1-(\phi-\phi_c)/(b-2\phi_c)]$ for $\phi_c\leqslant\phi\leqslant b-\phi_c$. When the atomic separation is in this range, a "weak bond" is said to exist. When the force is normalized to the shear modulus, the relation may be expressed as follows:

$$\begin{aligned}(F/k_2b)&=(\phi/b), && 0\leqslant(\phi/b)\leqslant\gamma;\\ &=-\alpha(\phi/b)+\gamma(1+\alpha), && \gamma\leqslant(\phi/b)\leqslant 1-\gamma;\\ &=0, && (\phi/b)\geqslant 1-\gamma,\end{aligned} \tag{2.12}$$

where $\gamma=(\phi_c/b)=(F_c/k_2b)=(\tau_c/\mu)$, $\alpha=\gamma(1-2\gamma)^{-1}$, τ_c = critical shear stress of perfect crystal. The solution will be carried out for a range of values of γ.

Because of the two types of force relations, Eqs. (2.12), the slip plane is divided into three regions, defined by (see Fig. 3):

$$\begin{aligned}&j\leqslant -M_2: && F_{jj}\text{ strong, }F_{j,j-1}=0;\\ &-M_2+1\leqslant j\leqslant M_1-2: && F_{jj}\text{ and }F_{j+1,j}\text{ weak;}\\ &j\geqslant M_1: && F_{j,j-1}\text{ strong, }F_{jj}=0.\end{aligned}$$

The constants M_1 and M_2 are defined by these relations; their value depends on the final displacement distribution, which would indicate a trial and error analysis. The actual procedure used is discussed below. In addition the force F_{ij}, $i=-M_2+1$, $j=-M_2$, may be weak or zero; the actual case will be denoted by giving δ_L the value 1 or 0, respectively. Similarly δ_R will denote whether F_{ij}, $i=j=M_1-1$, is weak or zero.

Now the relations (2.12) and (2.6) may be used in Eq. (2.10), together with Eqs. (2.8), and after some manipulation the two infinite, coupled systems of

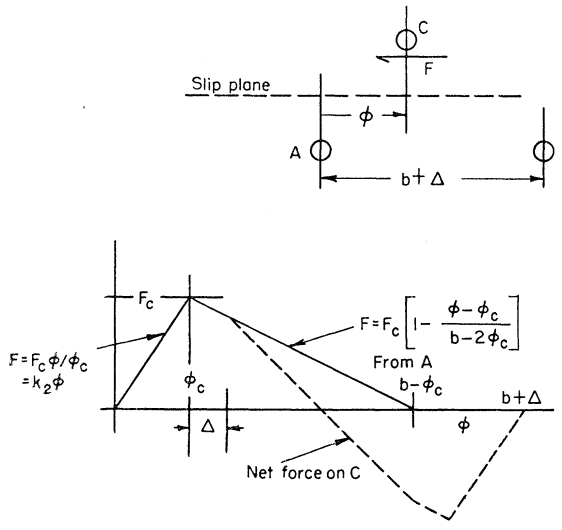

FIG. 2. Slip-plane force law. The upper figure shows three typical atoms, one above and two below the slip plane. The solid line in the graph shows the force of attraction (F) between atoms C and A as a function of the spacing (ϕ) between them. The dashed line shows the net force on C from both the other atoms. The manner in which this net force is changed by a change in spacing, Δ, between these two lower atoms is also shown.

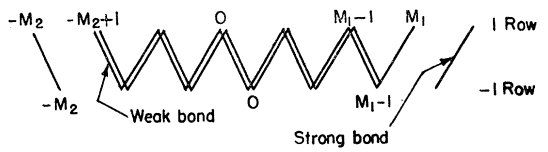

FIG. 3. Sample distribution of atomic bonds along the slip plane. M_2 and M_1 denote the atom numbers, counting from the center (atom 0), of the first atoms connected to strong bonds.

equations are derived:

$$\begin{aligned}\sum_{-\infty}^{\infty} k_{j-k}\varphi_k-(1+2R)\varphi_j+R(\varphi_{j+1}+\varphi_{j-1})&\\ =-V_j+\varphi_j-\psi_{j-1}-F_j-G_{j-1}, &\quad j\geqslant 1,\\ =-V_j-\sigma+F_{-1}-F_0, &\quad j=0,\\ =-V_j+\varphi_j-\psi_j+F_{j-1}+G_j, &\quad j\leqslant -1.\end{aligned} \tag{2.13a}$$

$$\begin{aligned}\sum_{-\infty}^{\infty} k_{j-k}\psi_k-(1+2R)\psi_j+R(\psi_{j+1}+\psi_{j-1})&\\ =W_j+\psi_j-\varphi_{j+1}+F_j+G_j, &\quad j\geqslant 0,\\ =W_j+\psi_j-\varphi_j-F_j-G_j, &\quad j\leqslant -1.\end{aligned} \tag{2.13b}$$

In these equations, $\varphi_j=\varphi_j'/b$, $\psi_j=\psi_j'/b$, $R=k_1/k_2$, with

$$V_j=V_j'/k_2b,\quad W_j=W_j'/k_2b, \tag{2.14}$$

and

$$\varphi_j,\psi_j\to 0\quad\text{as}\quad |j|\to\infty.$$

The effect of the weak bonds enters through the quantities F_j and G_j, which are defined as

$$\begin{aligned}F_j&=\bar{F}_j, && -M_2+1-\delta_L\leqslant j\leqslant M_1-2+\delta_R,\\ &=0 && \text{otherwise.}\end{aligned} \tag{2.15a}$$

$$\begin{aligned}G_j&=\bar{G}_j, && -M_2+1\leqslant j\leqslant M_1-2,\\ &=0 && \text{otherwise.}\end{aligned} \tag{2.15b}$$

with

$$\begin{aligned}\bar{F}_j&=\alpha[\psi_j-\varphi_{j+1}-\gamma-\sigma], && j\leqslant -2,\\ &=\alpha[\psi_{-1}-\varphi_0-\gamma-\sigma+\tfrac{1}{4}], && j=-1,\\ &=\alpha[\varphi_0-\psi_0-\gamma+\sigma+\tfrac{1}{4}], && j=0,\\ &=\alpha[\varphi_j-\psi_j-\gamma+\sigma], && j\geqslant 1;\end{aligned} \tag{2.16a}$$

$$\begin{aligned}\bar{G}_j&=(1+\alpha)[\psi_j-\varphi_j-\gamma-\sigma], && j\leqslant -1,\\ &=(1+\alpha)[\varphi_{j+1}-\psi_j-\gamma+\sigma], && j\geqslant 0.\end{aligned} \tag{2.16b}$$

where

$$\sigma=\tau/\mu=\tau b/k_2.$$

Equations (2.13), together with the definitions (2.15) and (2.16), constitute the mathematical problem. In the next section the method of computation of the constants k_j, V_j, and W_j is presented, together with a summary of the method of solution.

3. INFLUENCE COEFFICIENTS AND METHOD OF SOLUTION

The influence coefficient k_{ij} is defined as the displacement u_{2i} of the i atom of the second row, when the

displacement u_{1j} of the j atom of the first row is unity, and the other first-row displacements are zero. Because of the infinite extent of the lattice all the boundary atoms are equivalent, and $k_{ij}=k_{i-j}$; then k_i is the solution u_{2i}^0 of the following problem

$$R(u_{i,j+1}+u_{i,j-1}-2u_{ij}) + (u_{i+1,j}+u_{i-1,j}-2u_{ij})=0, \quad i>1, \quad (3.1)$$

with $u_{1j}^0=\delta_{j0}$ and $\lim_{i\to\infty} u_{ij}^0=0$ (δ_{jk} is the Kronecker symbol). By the use of a technique similar to that presented by Babuška *et al.*,[1] of the Fourier series transform, this problem can be reduced to the solution of an ordinary difference equation. To apply this technique, let

$$\bar{u}_i(z)=\sum_{-\infty}^{\infty} u_{ij}z^j, \quad |z|=1, \quad (3.2)$$

then multiply each equation of the set (3.1) by z^j and sum over j. By use of the identities

$$\sum_{-\infty}^{\infty} u_{i,j\pm1}z^j=\sum_{-\infty}^{\infty} u_{ij}z^{j\mp1}=z^{\mp1}\bar{u}_i(z), \quad (3.3)$$

the equation

$$\bar{u}_{i+1}-2\beta\bar{u}_i+\bar{u}_{i-1}=0 \quad (3.4)$$

is derived, where

$$\beta=1+R[1-\tfrac{1}{2}(z+z^{-1})],$$

$$\bar{u}_1(z)=\sum_{-\infty}^{\infty}\delta_{0j}z^j=1, \quad \lim_{i\to\infty}\bar{u}_i=0,$$

and z is limited to the unit circle.

The method is valid provided the series (3.2) converges for all i; this will be confirmed by the results, where it will appear that u_{ij}^0 is $0(j^{-2})$ as $|j|\to\infty$.

A solution to the present problem is obtained by taking

$$\bar{u}_i(z)=r^{i-1}(z), \quad (3.5)$$

and by using (3.4) to determine the form of $r(z)$. This satisfies the condition $\bar{u}_1(z)=1$, and will satisfy the requirement $\lim_{i\to\infty}\bar{u}_i(z)=0$ provided $|r(z)|\leqslant 1$ on the unit circle. By substitution of (3.5) into (3.4) we get

$$r^2-2\beta r+1=0, \quad (3.6)$$

which has the solutions

$$r(z)=\beta(z)\pm[\beta^2(z)-1]^{1/2}. \quad (3.7)$$

A brief investigation shows that $r=\beta-(\beta^2-1)^{1/2}$ is the correct choice. In fact, on the unit circle

$$\beta=1+R[1-(z+z^{-1})/2]=1+R(1-\cos\theta)\geqslant 1,$$

where

$$\theta=\arg(z), \quad 0\leqslant\theta\leqslant 2\pi.$$

Therefore,

$$\beta^2-1\geqslant\beta^2-1-2(\beta-1)=(\beta-1)^2,$$

so that $\beta-1\leqslant(\beta^2-1)^{1/2}$, and $r(z)$ is real on $|z|=1$ with $r(z)\leqslant 1$ there. It is also seen that $r(z)$ is symmetric $[r(-\theta)=r(\theta)]$ on $|z|=1$. It is of class C^∞, $0<\theta<2\pi$ and has a simple discontinuity in slope at $\theta=0$.

The influence coefficients now may be obtained by inverting the transform (3.2):

$$k_j=u_{2j}^0=(2\pi i)^{-1}\oint_{|z|=1} z^{-j-1}r(z)dz. \quad (3.8)$$

Finally, the displacements u_{2i} of the second row, for any prescribed distribution of first-row displacements u_{1j}, are found by

$$u_{2i}=\sum_{-\infty}^{\infty} k_{i-j}u_{1j}. \quad (3.9)$$

This formula is valid whenever the series converges. Since k_j, as shown below, is $O(j^{-2})$ as $|j|\to\infty$, the representation (3.9) is valid for any distribution for which u_{1j} is $O(1)$ for large j.

Before computing the k_j, we show how they may be related to the boundary forces V_j and W_j defined by the relations (2.11) and (2.14). By substitution of the conditions (2.4) into Eq. (2.8), with the use of the properties

$$k_{-j}=k_j \quad \text{and} \quad \sum_{-\infty}^{\infty} k_j=r(1)=1,$$

and then the substitution of the resulting expressions for u_{2j}^{II} and $u_{-2,j}^{\mathrm{II}}$ into Eqs. (2.11), the following results may be derived:

$$\begin{aligned} V_j&=\tfrac{1}{4}\{1-k_0-2\sum_{1}^{j-1}k_n-k_j\}, && j>1;\\ &=\tfrac{1}{4}\{1+R-k_0-k_1\}, && j=1. \end{aligned} \quad (3.10a)$$

$$\begin{aligned} W_j&=\tfrac{1}{4}\{1-k_0-2\sum_{1}^{j}k_n\}, && j>0;\\ &=\tfrac{1}{4}\{1+2R-k_0\}, && j=0; \end{aligned} \quad (3.10b)$$

and

$$V_{-j}=-V_j, \quad W_{-j}=-W_{j-1}.$$

Now from Eq. (3.8)

$$k_{-j}=k_j=(2\pi i)^{-1}\oint_{|z|=1} z^{j-1}r(z)dz. \quad (3.11)$$

Because of the nature of the function $r(z)$, $z^{j-1}r(z)$, for $j\geqslant 0$, is analytic $|z|\leqslant 1$ away from the cut $x_1\leqslant x=\mathrm{Re}(z)\leqslant 1$, where x_1 is the branch point of $r(z)$ inside the unit circle. Consequently the contour of integration in (3.11) may be contracted down to this cut, and the

integral then becomes,

$$k_j=(2\pi i)^{-1}\left\{\int_1^{x_1} x^{j-1}r^+(x)dx+\int_{x_1}^{1} x^{j-1}r^-(x)dx\right\}$$
$$=R(2\pi)^{-1}\int_{x_1}^{1} x^{j-2}(1-x)(x-x_1)^{1/2}(x_2-x)^{1/2}dx, \quad (3.12)$$

where $r^+(x)$ and $r^-(x)$ are the limiting values of $r(z)$ on the top and bottom of the branch cut, and $x_2=x_1^{-1}$. Then

$$k_0=1+R-\pi^{-1}[2R^{1/2}+2(1+R)\tan^{-1}R^{1/2}],$$
$$k_1=-\tfrac{1}{2}R+\pi^{-1}[R^{1/2}+R^{-1/2}+(R-R^{-1})\tan^{-1}R^{1/2}], \quad (3.13)$$
$$k_2=\pi^{-1}[4/3R^{1/2}+2/RR^{1/2}-2R^{-1}(1+R^{-1})\tan^{-1}R^{1/2}].$$

We next derive a recurrence relation which may be used to determine the values of k_j, $j>2$ from the above values of k_0, k_1, k_2. This is done by consideration of the identity

$$\int_{x_1}^{1}(d/dx)[(R/2\pi)x^{j-1}(1-x)^2(x-x_1)^{3/2}(x_2-x)^{3/2}]dx=0$$
$$=(j+4)k_{j+3}-[(3+4/R)j+(7+10/R)]k_{j+2}+[(3+4/R)j+(2+2/R)]k_{j+1}-(j-1)k_j,$$

which leads to the desired relation

$$k_{j-1}=[(3+4/R)-(5+6/R)j^{-1}]k_{j-2}-[(3+4/R)-(10+14/R)j^{-1}]k_{j-3}+(1-5j^{-1})k_{j-4}. \quad (3.14)$$

The relation (3.14) is, of course, analytically exact. It is poorly suited, however, for numerical computation of k_j for large j. Because the coefficients on the right-hand side are larger than one, any error tends to propagate exponentially, and since the k_j themselves decrease with increasing j, the relative error is even greater.

An asymptotic formula for k_j, for large j, may be obtained by use of a theorem from Lighthill.[18] His theorem 30, adapted to this case, reads: If $r(\theta)$ is a periodic generalized function, with one singularity in the period $-\pi<\theta\leqslant\pi$, such that $r(\theta)-F(\theta)$ has absolutely integrable Pth derivative in an interval including the singularity, where $F(\theta)$ is a linear combination of functions $|\theta|^p$, then k_j, the jth Fourier coefficient of $r(\theta)$, satisfies

$$k_j=(2\pi)^{-1}G(j/2\pi)+o(|j|^{-p}), \quad \text{as} \quad |j|\to\infty,$$

where $G(\omega)$ is the Fourier transform of $F(\theta)$. If $F(\theta)=\sum_p a_p|\theta|^p$, then $G(\omega)=\sum_p a_p 2(p!)(2\pi i\omega)^{-p-1}$.

[18] M. J. Lighthill, *Introduction to Fourier Analysis and Generalised Functions* (Cambridge University Press, New York, 1958), p. 72.

It was shown above that $r(\theta)$, $\theta=\arg(z)$, is in class C^∞ $-\pi<\theta\leqslant\pi$ except at $\theta=0$. Moreover, for large j, the Fourier coefficients of $r(\theta)$ are the same as those of $-(\beta^2-1)^{1/2}$, $\beta=1+R(1-\cos\theta)$. By use of the power series for $\cos\theta$, near $\theta=0$ $-(\beta^2-1)^{1/2}=a_1|\theta|+a_3|\theta|^3+\cdots$, where a_1, a_3, $\cdots$, are certain constants. Then, from the theorem,

$$k_j\sim(R^{1/2}/\pi)[j^{-2}-(3/4)(R-1/3)j^{-4}-(15/16)(R^2+2R-1/15)j^{-6}-(315/64)\times(R^3+5R^2/3+13R/15-1/315)j^{-8}]+O(j^{-10}). \quad (3.15)$$

For $R=1$ and $j=4$, the error is about 0.03%. For $R=5$ and $j=5$, the error is about 0.5%. By proper combination of formulas (3.13), (3.14), and (3.15), it is possible to calculate, for the range $1\leqslant R\leqslant 5$, the quantities k_j accurate to 5 significant figures or better, except near the juncture of the recurrence relation (3.14) and the asymptotic formula (3.15), at $j=4$ or 5, where 3 significant figures are obtained.

Now that the constants k_j, V_j, and W_j have been computed, the mathematical problem is completely defined. The approximate solution to Eqs. (2.13) is found by the method of reduction,[19] by discarding, that is, all equations and unknowns commencing with a certain one. Specifically, for an approximation of order N, we require that $\varphi_j=0$, $|j|>N$, $\psi_j=0$, $j>N-1$ and $j<-N$. Physically this corresponds to fixing the atoms on the slip plane, further from the dislocation center than a certain distance, to the configuration of Fig. 1(c) (no assumption is made about the atoms not in rows 1 and -1). After the reduction the system consists of $4N+1$ equations in as many unknowns.

Several techniques are used in the solution that considerably reduce the effort required. As a first step, the displacements φ_j and ψ_j are found for the case in which no weak bonds exist, and the strong bond distribution is fixed [the bond distribution is that of Fig. 1(c)]. For this, Eqs. (2.13) are separated into symmetric and antisymmetric parts, and the resulting coefficient matrices, two of rank $2N$ each, are inverted by partitioning.[20] By this procedure it is necessary to invert four matrices of rank N, with four matrix multiplications, for each value of R and N.

In the second step the correct distribution of weak bonds is determined for the stress-free equilibrium position. This is done by adding the weak bonds in pairs and testing the displacements after each addition. By treating $\bar{F}_j$ and $\bar{G}_j$ [Eqs. (2.16)] as primary variables, rather than φ_j and ψ_j, the only effect of adding a weak bond is to modify one column of the original coefficient matrix. The effect of this, in turn, on the solution may be easily computed, by the method outlined in Appendix A, without any new matrix inversion. Moreover it is

[19] L. V. Kantorovich and V. I. Krylov, *Approximate Methods of Higher Analysis* (P. Noordhoff, Ltd., Groningen, 1958), p. 25.

[20] V. N. Faddeeva, *Computational Methods of Linear Algebra* (Dover Publications, Inc., New York, 1959), p. 102.

not necessary to retain all the elements of the first solution, so that after the first step the order of approximation N does not enter the problem. While the first step was independent of γ, the second step must be performed for each value of this parameter.

In the third (and final) step the dislocation is moved through the lattice. To do this it is necessary to add weak bonds on the right and remove them on the left, and to observe the effect of the external stress σ on each new configuration. The bonds are added in a manner similar to that used in the second step; since, in each configuration, the dependence on σ is linear, the calculation is not excessive. Through a sequence of such bond modifications the dislocation may be moved through a cycle, from one equilibrium position to the next, an atomic spacing distant.

The procedure outlined above has been programmed for the IBM 1620 digital computer. The program can treat an order of approximation up to $N=20$, initial dislocation widths from $M_1=3$ to $M_1=7$, and values of R less than or equal to five. These limitations are somewhat arbitrary, being determined by machine capacity and speed and a compromise between program efficiency and flexibility. It is believed that these ranges adequately cover the regions of interest. The usual precautions were taken to ensure against error, including the use of internal program checks and a sample computation on the desk calculator.

The accuracy of the solutions obtained is discussed in Appendix B. The error in the values determined for the P-N stress, for order of approximation $N=20$, is believed to be less than 10^{-6}, including the effect of the truncation approximation, for stresses ranging from 10^{-5} to 10^{-3}.

4. RESULTS AND CONCLUSIONS

Results were obtained, with the 1620 computer, for values of R (the ratio of central to noncentral forces) equal to 1.0, 2.0, and 5.0. For each value of R, the parameter γ (the ratio of perfect crystal shear strength to shear modulus) was varied between the limits imposed by the maximum and minimum dislocation widths acceptable to the program. In general, the calculations were made with N (the order of approximation) equal to 20; in addition, certain representative cases were run for N equal 5 and 10, in order to obtain a measure of the convergence.[21]

Dislocation Width

The width of the dislocation is found by first counting the number of atomic distances, measured perpendicular to the line of the dislocation, contained in the region within which the displacement is less than one-half its limiting value. Linear interpolation is used when the half-displacement point lies between two atoms.

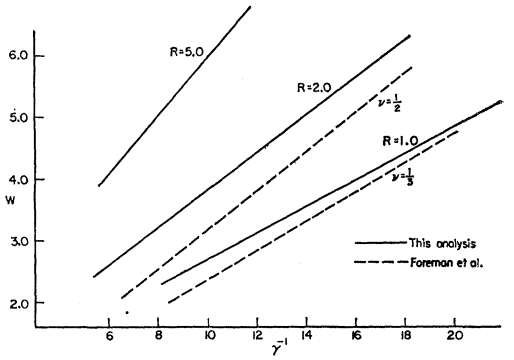

FIG. 4. Variation in dislocation width w, with normalized critical shear stress, γ [see Eq. (2.12)]. R is the ratio of central to noncentral forces [see Eq. (2.13)], while ν is the Poisson ratio in the continuum calculations.

The width is then taken as this number of atomic distances multiplied by b.

Figure 4 shows the variation of w with $1/\gamma$; the straight lines fit the computed values very closely (± 0.02 in w). This is the relationship found by Foreman, Jaswon, and Wood,[9] and for comparison the results of the latter paper are plotted for several values of ν, the Poisson ratio. The widths, and their variation, are seen to be comparable.

Dislocation Motion

Figure 5 shows the various details in the motion of a dislocation through a cycle, for one of the patterns observed.[22] The basic graph [Fig. 5(a)] shows the variation of stress σ with dislocation displacement d. In all cases this variation was periodic over an atomic spacing, but the patterns differed as to whether the initial configuration was stable, which occurred in about half the cases, and as to whether one or two stable configurations existed in each cycle. The situation predicted by Peierls,[6] in which the initial position is unstable and each cycle has two stable positions, occurred for only a few values of the parameters and for the lowest P-N stresses. On the other hand, Huntington's prediction,[11] that each cycle should have only one stable position, was generally borne out.

Figure 5(b) shows, in addition, the bond configuration, along the slip plane, valid for each portion of the motion.

In Fig. 5 the initial distribution is stable—a positive stress corresponds to a positive displacement— and valid until either the G_2 bond [see Fig. 5(b)] becomes weak, or until the F_{-3} bond disappears. As the figures indicate, the former takes place first, and then the F_3, F_{-3} bonds must be checked for the next step. In the first change a strong bond is replaced by a weak one, and consequently the dislocation moves more easily—the rate of increase of displacement with stress is

[21] These last results are discussed in Appendix B.

[22] Six different patterns were observed, in each of which the sequence of bond changes was different.

greater. Next an extra bond is added on the right (F_3) and again the rate of motion increases; in this portion of the cycle the stress must be lowered to maintain equilibrium as the displacement increases. The configuration is now metastable; if the stress is relaxed to zero, the bond arrangement is still valid, but in a dynamic analysis the dislocation would tend to jump forward or back to a stable position. The rest of the cycle is a mirror image of the first half, until the original distribution, displaced to the right by one atom spacing,

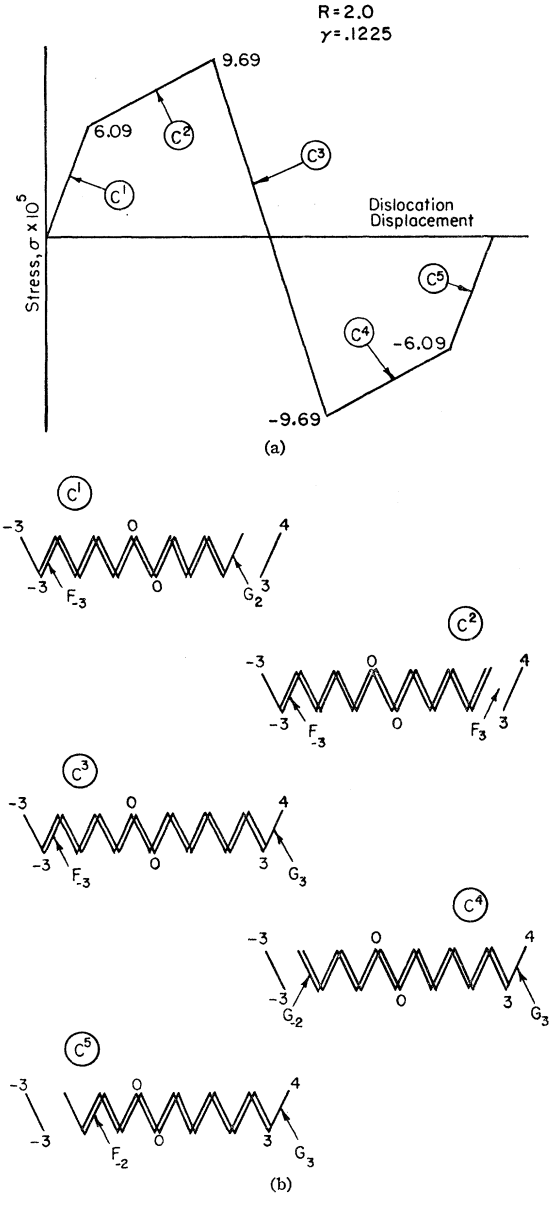

FIG. 5. (a) Stress cycle. Variation in external stress σ, required to maintain equilibrium as the dislocation moves forward one atom spacing. (b) Bond configuration, along the slip plane, valid for the different straight line portions of the stress cycle of (a). The symbols F_j and G_j are used in the text to designate particular bonds.

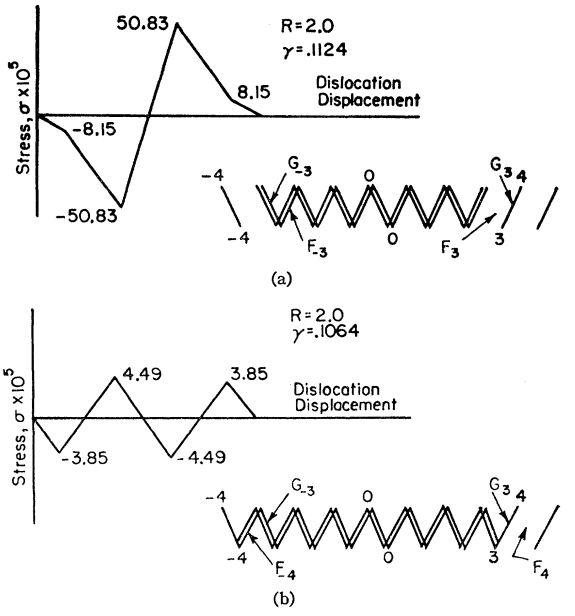

FIG. 6. Typical stress cycles. Initial bond configurations are also shown.

is attained. The P-N stress for this cycle, 9.69×10^{-5}, is reached at the second turning point.

Stress cycles and initial bond distributions for two patterns are presented in Fig. 6. The sequence of bond changes for the cycle of Fig. 6(a) is F_3, G_{-3}, G_3, F_{-3}; the P-N stress, 50.83×10^{-5}, can be determined from the stress at the second bond change. The cycle in Fig. 6(b) is attained through the sequence F_{-4}, G_3, G_{-3}, F_4; this is one of the few cases, mentioned earlier, that has two stable positions in the cycle, and the P-N stress, 4.49×10^{-5}, is much lower than that for neighboring values of γ.

Peierls-Nabarro Stress

The results of the calculation of the P-N stress are shown in Fig. 7, in which σ_{PN} is plotted against $1/\gamma$ for $R=2.0$. The most striking feature of the variation of σ_{PN} is its periodic nature; apart from this, however, the stress decreases almost exponentially

$$\sigma_{PN} \propto e^{-0.3/\gamma} \propto e^{-w}, \tag{4.1}$$

where the relation between γ and the width w is derived from Fig. 4. The exponential factor differs considerably from the dependence

$$\sigma_{PN} \propto e^{-2\pi w} \tag{4.2a}$$

projected from Peierls' calculation,[23] and from

$$\sigma_{PN} \propto e^{-4\pi w} \tag{4.2b}$$

computed by Foreman, Jaswon, and Wood,[9] for the continuum model.

[23] See reference 5, p. 64.

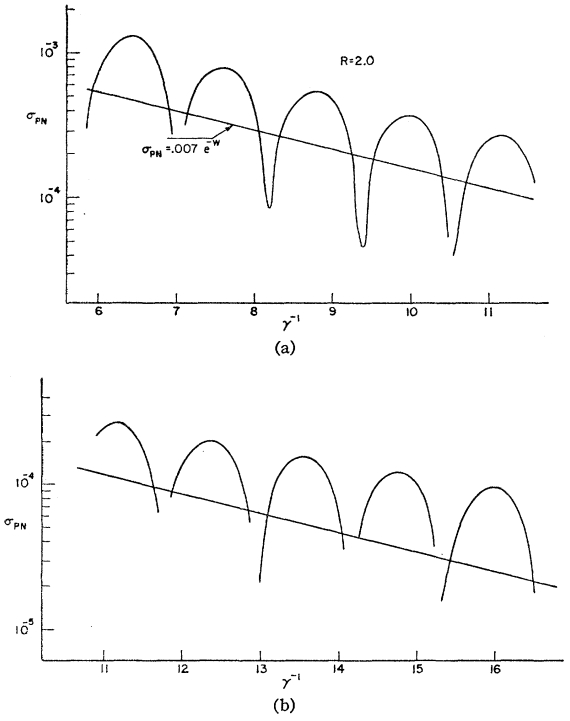

FIG. 7. Variation of P-N stress σ_{PN} with the normalized critical shear stress, γ. The straight line shows the estimated average stress as function of dislocation width w (see Fig. 4).

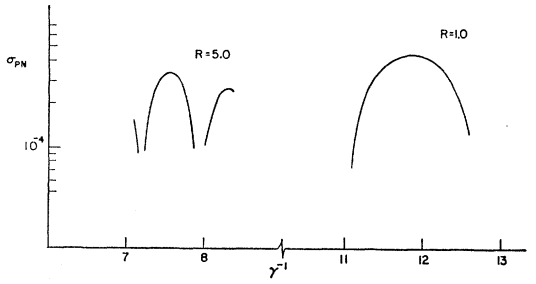

FIG. 8. Variation of σ_{PN} with the normalized critical shear stress γ for two additional values of R, the ratio of central to noncentral forces in the crystal model employed.

Although a definitive statement must await further improvement in the model, it would seem that relation (4.1), since it is derived from a direct force calculation on a discrete model, may be, in spite of the highly idealized nature of the model, more realistic than (4.2).

The large number of points needed to define the curve in Fig. 7 (70 were used) made a similar definition for $R=1.0$ and 5.0 unfeasible. Figure 8 shows a single cycle for each of these values, and indicates the effect of R on the period of the variation.

The variation may be explained qualitatively by a discussion of the mobility of the dislocation and the critical points in its motion:

The mobility of the dislocation is determined roughly by the number of weak bonds, and by the spring constant of these bonds. These negative springs amplify the effect of the external stress, and cause the relatively large displacements near the center. As γ decreases, the effect of each of the weak bonds decreases steadily (see Fig. 2, with $\gamma=\phi_c/b$), while the number of these bonds increases in steps. On the other hand, the distance the dislocation must move to reach a critical point, a point at which the bond configuration changes, depends on the amount that the initial spacing of the two critical atom pairs differs from ϕ_c or $b-\phi_c$, and this too changes steadily with γ.

These two effects, variation in mobility and in proximity of critical points, together cause the cyclic nature of the Peierls-Nabarro stress. In Fig. 7 the point $\gamma^{-1}=9.4$, for example, is a state of high mobility, due to the particular bond distribution and strength; therefore, although the dislocation, initially, is not near a critical point, the P-N stress is low. From this point to the point $\gamma^{-1}=10.0$ the mobility decreases with γ and, although the critical point is initially closer, the P-N stress increases. From this second point to the point $\gamma^{-1}=10.6$ the mobility continues to decrease, but the effect of the proximity of the critical point becomes dominant. After this point the bond distribution valid in the beginning changes; the new stable distribution, since it has more weak bonds, is again highly mobile, and the cycle repeats.

The amplitude of these cycles is undoubtedly magnified by the type of force law chosen, since, for this law, any bond must be either weak or strong and the spring constants of the two types differ radically. For any force law, however, the number of "weak" bonds, and their "spring constants," must change with γ, or its equivalent, and some alternation in the rate of change of the Peierls stress with width might be expected.

In conclusion, the previous results will be summarized briefly: An analysis of a straight edge dislocation in an idealized, infinite, simple cubic lattice has shown that

(1) The width of the dislocation has the same relation to the force law as that found previously,[9] and stands in rough quantitative agreement with these previous results (see Fig. 4).

(2) The Peierls-Nabarro stress, for the same force law, is similar to that found by Peierls and Nabarro,[6,7] but the rate of decrease of this stress with increasing width is much less than previously assumed (see Fig. 7).

(3) The P-N stress, in this model, exhibits a cyclic variation of short period and large magnitude as the force law is changed.

ACKNOWLEDGMENT

The author finds it a great pleasure to thank Professor J. H. Weiner for suggesting this problem, and for his continuous interest and invaluable guidance during this work.

APPENDIX A

For the matrix equation

$$Ax^0=c,$$

where A is a square matrix and x^0 and c are column vectors, the solution is, of course,

$$x^0=A^{-1}c.$$

If now the matrix A is modified by adding the vector a to the pth column, so that the equation becomes

$$Ax^1+ax_p{}^1=c,$$

where $x_p{}^1$ is the pth element of the vector x^1, direct substitution will verify that

$$x^1=x^0-x_p{}^0(1+a_p{}^0)^{-1}a^0,$$

where $a^0=A^{-1}a$. Consequently, if, in the initial inversion, $A^{-1}a$ as well as $A^{-1}c$ is obtained, it is a simple matter to obtain x^1. Also, if only a few elements of x^1 are required, only the corresponding elements of x^0 and a^0 (including the pth) need be retained.

Similarly, if the equation now becomes

$$Ax^2+ax_p{}^2+bx_q{}^2=c,$$

then

$$x^2=x^1-x_q{}^1(1+b_q{}^1)^{-1}b^1,$$

where

$$b^1=b^0-b_p{}^0(1+a_p{}^0)^{-1}a^0,$$

and

$$b^0=A^{-1}b.$$

That is, in the initial inversion $A^{-1}c$, $A^{-1}a$, and $A^{-1}b$ are obtained, and only the desired elements retained, while in the first modification both x^1 and b^1 are derived in the same way. The technique may clearly be extended to the modification of any number of columns of the original coefficient matrix.

APPENDIX B

Two possible sources of error were foreseen: truncation error, due to the use of only a finite number of equations and unknowns in the solution; and round-off error, since only a fixed number of digits (8) were carried in the calculation. Certain intermediate data were used to determine that this latter error was unimportant, and the high regularity of the results confirm this, since this error should be of random nature.

The first source of error, truncation of the infinite system, was evaluated by running a number of cases at different orders of approximation. The convergence is generally quite good; Table I shows the variation in width and P-N stress. The main effect of the truncation, which physically corresponds to pinning the atoms of the slip plane further from the center than a certain distance, was to impose a certain resistance to the motion of the dislocation, similar to the effect of a row of impurity atoms. This resistance could be detected

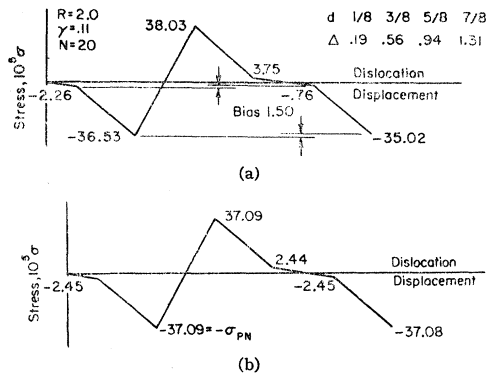

FIG. 9. (a) Stress cycle, indicating resistance imposed by truncation for order of approximation $N=20$. Δ is the truncation error when the dislocation has moved through the fraction d of one atom spacing. (b) Stress cycle, with bias Δ removed.

and removed by the observation of a certain "bias" in the periodicity of the stress, as shown in Fig. 9(a). This bias was almost independent of γ, and was not large for order of approximation $N=20$, as indicated in Table I. It was removed by arbitrarily assuming that the changes in slope of the stress-displacement relation occurred at $d=1/8$, $3/8$, $5/8$, and $7/8$, and by subtracting these fractions of the bias at each turning point, as illustrated in Fig. 9(b). All values of the P-N stress presented here have had this effect removed.

TABLE I. Effect of truncation on the width and P-N stress.

R	γ	N	$10^5\sigma_{PN}$	w	Bias/cycle
1.0	0.12	5	113.83	2.35	66
		10	108.28	2.36	6.2
		20	107.76	2.36	0.71
	0.05	10	6.16	4.85	8.4
		20	7.06	4.86	0.75
2.0	0.16	5	107.98	2.65	149
		10	112.22	2.66	13.2
		20	112.55	2.66	1.48
	0.06	10	2.15	5.79	22.7
		20	2.50	5.83	1.61
5.0	0.19	5	73.52	3.57	570
		10	75.58	3.75	41
		20	77.51	3.78	4.1
	0.09	10	8.13	6.41	73
		20	7.62	6.49	4.5

This bias is felt to be a measure of the loss of accuracy due to truncation, and can, therefore, be used to estimate this error. At $R=2$ this correction to the P-N stress is 0.19×10^{-5} at the first turning point, and 0.56×10^{-5} at the second. If the correction itself is assumed known to within 20%, then the error in the P-N stress is not greater than 0.1×10^{-5}. This represents a relative error of 1% for $\sigma_{PN}=10\times10^{-5}$, and, for $\sigma_{PN}=1\times10^{-5}$, which is lower than any observed, only 10%.